ANALES DE MECANICA DE LA FRACTURA VOL. 16 (1999)

FATIGUE LIFE TIME PREDICTION OF AUSTENITIC STAINLESS STEEL COMPONENTS

F. De Backer°, V. Schoss°, L. Baer+, G. Maussner°
° Siemens AG, KWU NT11
+ Siemens AG, ZT MF1
Freyeslebenstrasse 1, 91058 Erlangen, Alemania

Resumen. El daño sufrido por los componentes de aceros austeníticos en fatiga es uno de los mayores problemas en las centrales nucleares. El objetivo del presente estudio es, por un lado, la caracterización de las propiedades, tanto microestructurales, como mecánicas y físicas, de los aceros austeníticos sometidos a una deformación por fatiga y con vida residual definida. Y, por otro lado, el desarrollo y la calificación de métodos de ensayo no destructivos, susceptibles a los cambios en las propiedades del material, con el fin de determinar la vida residual de los componentes estructurales. Se han ensayado probetas de fatiga para establecer una correlación entre los parámetros de fatiga y los cambios microestructurales que ocurren antes de la iniciación de microgrietas. En particular, se estudia la formación de la martensita inducida por deformación y se evalúan los cambios relacionados en las propiedades magnéticas. Los resultados demuestran la sensibilidad de los diferentes métodos de ensayo no destructivos para evaluar la vida residual en fatiga.

Abstract. A mayor problem in nuclear power plants is the fatigue damage of austenitic steel components. The aim of the present study is, on the one hand, the characterisation of austenitic stainless steels (microstructure, mechanical and physical properties) with defined fatigue strain and residual life time and, on the other hand, to develop and qualify non-destructive testing methods, which are sensitive for the changes of the properties, to determine the residual life of structural components. Tensile fatigue specimens were tested to establish a correlation between fatigue parameters and the changes in microstructure, that occur before the initiation of microcracks. In particular the volume fraction of deformation induced martensite and the related changes in magnetic properties have been considered. The results show the sensitivity of different non-destructive testing methods for the evaluation of the usage factor.

1. INTRODUCTION

In view of plant life extension efforts of nuclear power plants many investigations are going on to assess the structural integrity of different components. A large proportion of the defects developing or propagating in components during operation is caused by cyclic loading. Materials subjected to cyclic loading exhibit changes in microstructure already before crack initiation begins, this period covers a considerable part of the fatigue life. Therefore, operational monitoring and early detection of incipient damage caused by cyclic loading is extremely important.

The fatigue behaviour of austenitic steel depends on material composition and history, loading conditions and temperature. During fatigue loading of austenitic steel microstructural changes occur, which affect both the mechanical and physical material properties. Typical features are the rearrangement of dislocations and in some cases a deformation induced martensitic transformation. Those microstructural changes depend on the applied load level, life time and temperature [1, 2]. One of the aims of the present study is the correlation of the fatigue loading conditions and residual life time with these microstructural phenomena. In particular the formation of deformation induced martensite is analysed, which is accompanied by pronounced changes in the magnetic properties. Therefore different non-destructive testing methods (NDT) are applied and their sensitivity is compared.

Tensile fatigue specimens are strained at different load levels to defined usage factors in the range of low cycle fatigue (LCF) up to high cycle fatigue (HCF). The material properties and the microstructure are characterised by metallography, microhardness testing, x-ray diffraction, and eddy current systems, both conventional and a SQUID (Superconducting Quantum Interference Device). The microstructure is investigated with a transmission electron microscope (TEM), in order to examine the appearance and arrangement of crystal defects, in particular the formation of a dislocation cell structure and glide bands.

2. MATERIALS

The materials used in this study are austenitic stainless steels chosen for their relevance in nuclear power plant piping and because of their instability properties of the

austenitic phase. Two stainless steels are Nb stabilised, corresponding to the German grade 1.4550 (equivalent to AISI 347), denominated Nb-I and Nb-II in this paper. The third steel is Ti stabilised, corresponding to the German grade 1.4541 (equivalent to AISI 321), denominated Ti-I. The mechanical properties and chemical composition are represented in Table 1 and 2, respectively.

Table 1. Mechanical properties

Material	Yield Stress (MPa)	Tensile Strength (MPa)	Micro-hardness (HV0,2)	Grain Size (μm)
Nb-I	221	608	172	30
Nb-II	262	649	198	25
Ti-I	207	555	140	95

Table 2. Chemical composition

Material	%C	%Si	%Mn	%Cr
Nb-I	0,027	0,24	1,91	17,55
Nb-II	0,03	0,68	1,65	17,18
Ti-I	0,035	0,62	1,13	17,29
%Ni	%Ti	%Mo	%Nb+%Ta	%N
9,2	0,005	0,038	0,525	0,0255
9,19	-	0,47	0,67	0,038
10,65	0,23	-	-	0,02

3. EXPERIMENTAL PROCEDURE

Several cylindrical fatigue specimens with a 6 mm diameter are machined of all the studied materials.

3.1. Quasi-static tensile tests

To analyse the materials susceptibility to form deformation induced martensite, quasi-static tensile tests are carried out. During the tests the evolution of the volume fraction of magnetic content is measured.

3.2. Fatigue tests

The Nb-I steel specimens are tested under strain control in the LCF range ($N_f=10^3$-10^4). To evaluate the material properties during the fatigue life, several tests, with a determined strain amplitude, are stopped before failure of the specimen occurred. The specimens from the Nb-II and Ti-I steels, are tested under stress control in a range from LCF ($N_f=10^4$) to HCF ($N_f=10^7$). All stress controlled tests are run until fracture. All test are carried out at room temperature with load ratio, R=-1, the frequency varied between 0,1 and 6 Hz providing that no considerable heating due to plastic straining occurred. Table 3 summarises the load conditions and the number of fatigue cycles of the tested specimens.

Table 3. Load conditions and number of cycles of the tested specimens

Strain controlled

Specimen	Nb-I-13	Nb-I-7	Nb-I-6	Nb-I-5
$\Delta\varepsilon_t$ (%)	1,0	1,2	1,2	1,2
$N_{(f)}$	22874	25	50	801
Specimen	Nb-I-4	Nb-I-3	Nb-I-2	Nb-I-8
$\Delta\varepsilon_t$ (%)	1,2	1,2	1,2	1,5
$N_{(f)}$	1602	3205	6411	4370

Stress controlled

Specimen	Nb-II-4	Nb-II-2	Nb-II-3	Nb-II-5
$\Delta\sigma_a$ (MPa)	226	230	230	240
N_f	>10,5 10^6	612760	670740	447580
Specimen	Nb-II-7	Nb-II-9	Nb-II-8	Nb-II-10
$\Delta\sigma_a$ (MPa)	241	262	276	303
N_f	378510	118570	76160	27200

Sp.	Ti-I-5	Ti-I-7	Ti-I-4	Ti-I-3	Ti-I-8
$\Delta\sigma_a$	185	205	209	242	252
N_f	>12,3 10^6	270000	171020	12790	9470

3.3. Ferritscope measurements and X-ray diffraction

Magnetic phase measurements are carried out with a commercial Ferritscope (Feritscope, *Fischer*). This eddy current based instrument permits the measurement of the volume fraction of magnetic content at every moment of the test. Also X-ray diffraction is used to detect the presence of martensite after the fatigue test, at the fracture surface, at the specimen surface and in the volume.

3.4. Metallography and electron microscopy

After the test the specimen surface is analysed with a scanning electron microscope (SEM) to detect secondary cracks. Afterwards, cylinders and discs are cut, out of the broken specimen, for the metallographic study, the hardness measurements, the NDT-methods and the TEM. The microstructure of the fatigued steel is observed with a 200 kV TEM and electron diffraction patterns are obtained to identify the different phases.

3.5. SQUID and Elotest

A SQUID is a very sensitive magnetic flux sensor [3]. This is necessary because the volume fraction of magnetic phase depends on the stability of the austenitic steel and can be very low for specific conditions. The SQUID device is arranged to measure differences in magnetic properties between a tested and a reference specimen. The SQUID device, illustrated in Figure 1, consists of a specimen holder for the reference and the tested specimen, an excitating field generator, a high temperature SQUID and the corresponding electronics.

The excitation field coils and the antennas are situated at the bottom of the specimen holder holes. The system measures the difference of the excitated fields due to the eddy currents in both specimens. This means that the output is proportional to the difference in impedance of the reference and tested specimen, which is related with the magnetic properties of the material. In this case the SQUID is a very low noise amplifier for the antenna output, which provides a high sensitivity.

Measurements are also carried out with a commercial device, Elotest PLE (*Rohman*), developed for conventional eddy current measurements. The same specimen holder is used and the measurement method is similar to the SQUID, except here the antenna output is amplified with conventional electronics.

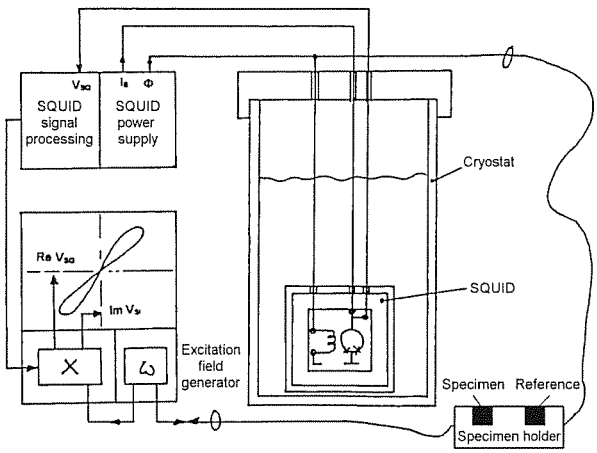

Figure 1. Eddy current measuring device with SQUID

4. RESULTS AND DISCUSSION

4.1. Quasi-static tensile tests

The evolution of the magnetic content measured with the Ferritscope in function of the plastic strain is shown in Figure 2. One can observe the much stronger tendency of the Nb-I and Nb-II steels to form deformation induced martensite compared to the Ti-I steel. It is also observed that no martensite is formed before a defined plastic strain, of about 15 to 20%, is attained.

4.2. Fatigue tests

During the strain controlled test of the Nb-I specimens an increasing stress amplitude until rupture is observed, as illustrated in Figure 3. A strong increase of σ_{max} occurs at about 1000 cycles for the specimens tested with $\Delta\varepsilon_t$=1,2%. This hardening of the material can be related to the formation of deformation induced martensite, as discussed in the next section.

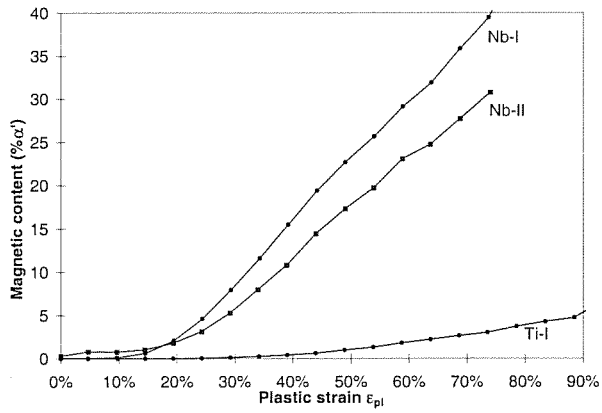

Figure 2. Evolution of the magnetic content in function of the plastic strain, during the quasi-static tensile tests

For some of the stress controlled tested Nb-II and Ti-I specimens the evolution of the total strain amplitude is shown in Figure 4 and 5, respectively. After an initial hardening during approximately the first 10 cycles (not represented in the Figures) the strain amplitude increases for both materials. This softening continues until rupture for the Ti-I steel, except for specimen Ti-I-5 which did not fail after more than 10^7 cycles. For the Nb-II steel, nevertheless, a secondary hardening is observed, which can be related to the formation of martensite.

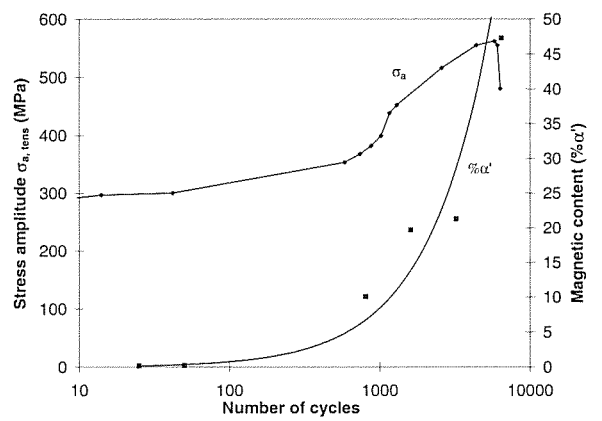

Figure 3. Stress amplitude and magnetic content evolution for strained controlled test of Nb-I

4.3. Ferritscope measurements and X-ray diffraction

A first observation that can be made is that the volume fraction of deformation induced martensite (%α'), formed during fatigue, varies over several orders of magnitude for the three materials. The value of %α' at rupture lies between 20-50%, 2-7% and <0,4% for the Nb-I, Nb-II and Ti-I steel, respectively. A second observation is that this value of %α' at rupture, measured on the specimen surface, increases with increasing maximum strain amplitude or load, as illustrated in Figure 6 for the Nb-II and Ti-I steels. The latter means that there exists no determined maximum

value of %α' at which the specimen fails.

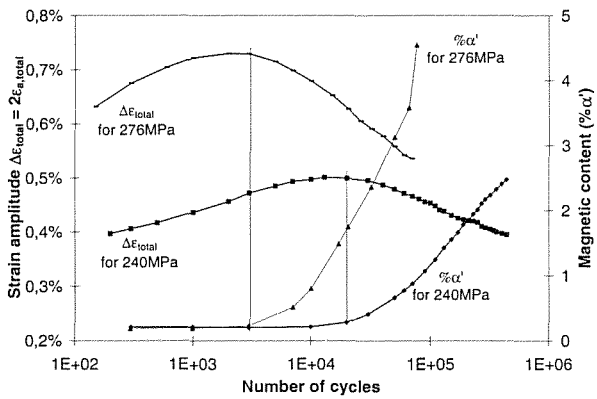

Figure 4. Total strain amplitude and magnetic content evolution for stress controlled test of Nb-II

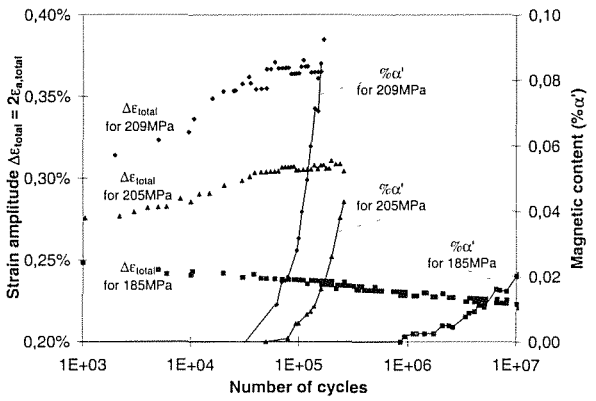

Figure 5. Total strain amplitude and magnetic content evolution for stress controlled test of Ti-I

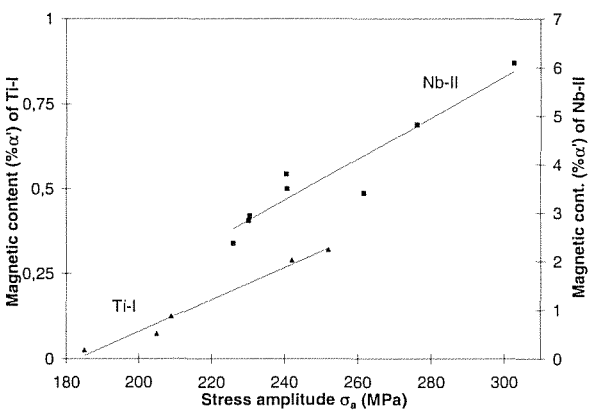

Figure 6. Value of %α' measured on the specimen surface at rupture for Ti-I and Nb-II

The evolution of %α' during fatigue is shown in Figures 3 and 4 for Nb-I and Nb-II specimens, respectively. For all the specimens, the evolution presents an incubation period (≅5% of fatigue life), afterwards the %α' increases continually until rupture. Comparing the evolution of the stress or strain amplitude with the %α' content, one can observe that the hardening of the material coincides very well with the strong increase of the martensitic content. For the Ti-I steel very low levels of %α' are attained during the tests, as illustrated in Figure 5, which makes the Ferritscope measurements less reliable. Nevertheless, after an incubation period the %α' increases and at that moment the softening of the material stops.

The presence of martensite on the fracture surface, observed with X-ray diffraction, is found to be independent of the load conditions for al tested specimens. For the Nb-I steel, the amount of martensite measured in the volume shows an almost linear correlation with the number of cycles. For the Nb-II steel an increase of the %α' in function of the fatigue load is observed, but the X-ray results show considerable scatter. For the specimens of the Ti-I steel, no martensite was detected in the volume with this technique. At the specimen surface, clear peaks corresponding to martensite could be identified for the Ti-I specimens. Nevertheless, due to the low α' content of the Ti-I specimens no useful quantitative results could be obtained with X-ray diffraction.

4.4. Metallography and electron microscopy

With the SEM secondary cracks could be observed on the LCF specimens. While on the majority of the HCF specimens only one crack initiated and propagated until final rupture occurred. As secondary cracks did not appear in all the specimens, they were of no use for a quantitative assessment of the residual life.

The optical metallographic analysis revealed that the fatigue specimens present a deformed microstructure with a higher concentration of slip bands and twins than in the as-received condition. Nevertheless, no clear quantitative difference is observed comparing with the transversal section of the as-received material. On the longitudinal section strong deformed grains near the fracture surface are visible. Only for the LCF specimens of Ti-I secondary cracks, starting at the surface, are observed.

In the as-received condition of the studied materials the dislocations are homogeneously distributed and dislocation clusters are pinned at carbides. Furthermore, stacking faults and dislocation pile-ups are frequently observed in the Ti-I steel.

Due to fatigue a dislocation generation and rearrangement takes place and more or less regular patterns are formed. For the Nb-I steel, the evolution of the dislocation arrangement is analysed for different stages of the fatigue life. Dislocation bands are already formed after only 25 cycles and for 50 cycles dislocation cells start to form. Furthermore, the cell walls get more and more sharper defined and the centres of the cells become free of dislocations, a disorientated subgrain structure is formed. For higher N, the cell

diameter (0,5-1,5 μm) decreases only slightly and the cells tend to transform from a globular aspect to a more elliptical form. Figure 7 shows an example of a fully developed dislocation cell structure.

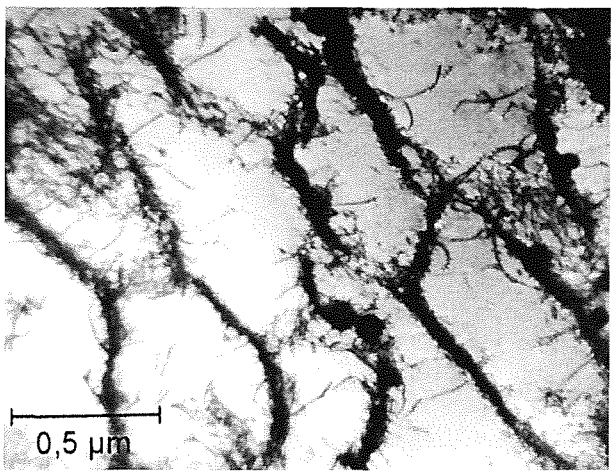

Figure 7. Dislocation cell structure after 3205 cycles, specimen Nb-I-3

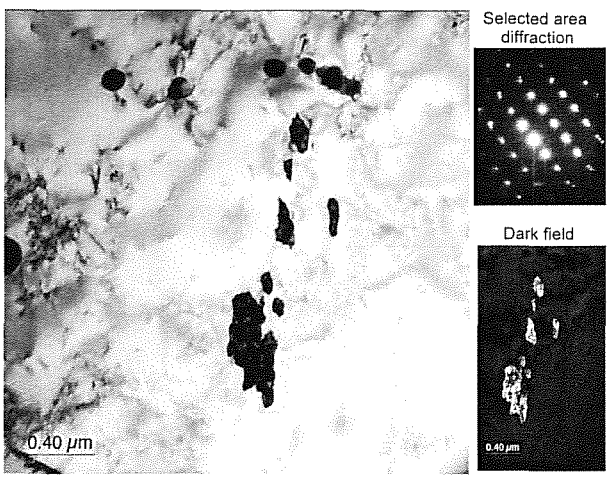

Figure 8. Martensite island with the diffraction pattern and dark field image, specimen Nb-II-2

At the end of the fatigue life of the Nb-II and Ti-I specimens, cells are observed for loads higher than 270 and 205 MPa, respectively, which correspond with the yield stress. For lower loads only dislocation veins or waves are observed. It is interesting to mention that also for specimen Nb-II-4 and Ti-I-5, who did not fail after more than 10^7 cycles, well defined dislocation veins lying parallel in a grain, are observed. This indicates that significant microstructural changes, with respect to the as-received state, take place before cracks are initiated. An example of a deformation induced martensite island is shown in Figure 8 with the corresponding diffraction pattern and dark field image.

4.5. Hardness measurements

The evolution of the hardness of the Nb-I specimens in function of the number of cycles demonstrates the hardening of the material during fatigue. The latter correlates with the evolution of the stress amplitude and the %α' evolution, represented in Figure 3. At rupture a mean hardness as high 280 HV0,1 is measured in the volume.

For the Nb-II and Ti-I steel hardness data are only available at rupture. On a microhardness profile of a longitudinal section one can observe the considerable increase at the fracture surface region, with respect to the as-received state; for both steels values up to 290 HV0,2 are measured. This is related with the enhanced formation of strain induced martensite in the crack surroundings. The hardness decreases to a constant value at about 2,5 mm from the fracture surface. This hardness value of the volume is slightly higher than the as-received hardness and also increases with the maximum fatigue load. Nevertheless, as the martensite content in the volume is relatively low, the hardness of the volume is not considerable higher than the as-received hardness, therefore no reliable correlation can be found between the hardness measurements and the load conditions.

4.6. SQUID and Elotest

The output signal of the SQUID measurements (the amplitude and the phase of an AC voltage) can be considered as a vector in the complex phase plane. The vector is determined by the vector length, R, corresponding to the voltage amplitude and phase angle, θ, the phase deviation, measured with respect to a reference state (for example the as-received state).

Figure 9 represents the evolution of the vector length R in function of the number of cycles for the Nb-I specimens ($\Delta\varepsilon_t$=1,2%), the evolution of the phase angle (not represented) has a similar aspect. The results show a clear correlation between the fatigue life and both vector parameters. For the Nb-II steel the vector length correlates very well with the applied load, over the total load spectrum used, as illustrated in Figure 10. Nevertheless, the phase angle (not represented) seams to saturate for an applied stress amplitude higher than 250 MPa, (%α'≥4% in Figure 6). Finally, for the Ti-I steel the evolutions of both vector parameters, R and θ, are represented in Figure 11. For such low %α' values, no clear relation is found between the R-values and the applied load, while the evolution of the phase angle does show a monotone increase with the applied load.

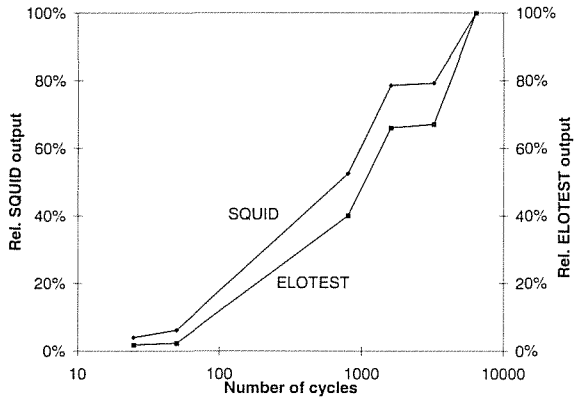

Figure 9. SQUID and Elotest output in function of fatigue life for Nb-I

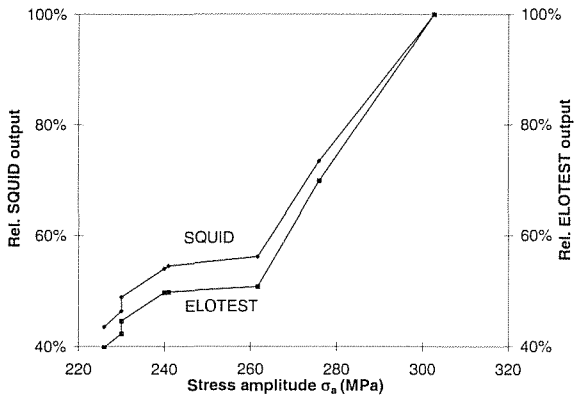

Figure 10. SQUID and Elotest output in function of applied load for Nb-II

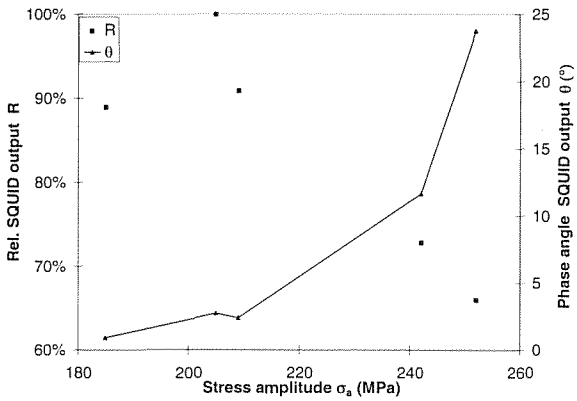

Figure 11. SQUID output in function of applied load for Ti-I

The results measured with the Elotest are also represented by a vector, as for the SQUID results. The results for Nb-I and Nb-II are represented in Figures 9 and 10, respectively. One can observe that no significant difference exists between the evolution of the vector lengths of both methods. The evolution of θ, measured with the Elotest, saturates for a lower magnetic content (%α'≅1%) than in the case of the SQUID measurements. For the Ti-I steel, the evolution of R obtained with the Elotest is similar as for the SQUID, no clear trend is observed, neither the evolution of θ does show any clear correlation with the load or magnetic content.

5. CONCLUSIONS

The results of the examinations indicate that, in the materials considered in the study, the evolutions of characteristic changes in the microstructure and the physical and mechanical properties are correlated to the fatigue straining of the material. At room temperature, the formation of martensite occurs, which can be measured non-destructively by sensitive magnetic analysis.

It is possible to correlate the non-destructive measurements obtained with the Ferritscope with the fatigue life of a specific material if the load conditions are known. The same conclusion is valid for X-ray diffraction, if the martensitic content is higher than 10%.

If martensite is formed during cyclic deformation, hardening of the material occurs. Determination of the fatigue state with hardness measurements is possible if the content of deformation induced martensite is high enough (>10%) to produce a significant hardness increase in the material volume and not only in the crack surroundings.

Identification of the fatigue state with a SQUID or conventional eddy current device (Elotest) is possible, if the content of deformation induced martensite is higher than 1%. For lower contents the phase angle evolution of SQUID response may be applied, but more test are necessary for confirmation.

6. REFERENCES

[1] Baudry, G. and Pineau, A., "Influence of Strain-induced Martensitic Transformation on the Low-Lycle Fatigue Behavior of a Stainless Steel", Mater. Sci. Eng., 28, 1977, pp. 229-242.

[2] Bayerlein, M., Christ, H.-J. and Mughrabi, H., „Plasticity-Induced Martensitic Transformation During Cyclic Deformation of AISI 304L Stainless Steel", Mater. Sci. Eng., A114, 1989, pp. L11-L16.

[3] Bär, L., Daalmans, G.M., Becker, E., Lohmann, H.P. and Mück, M., "SQUID Eddy Current Technique Applying Conformable Eddy Current Probes", 7th European Conference on Non-Destructive Testing, Copenhagen 1998, Proceedings Vol. 3, pp. 2555-2562.